

EFFECTS OF SOIL MOISTURE ON SIMULATED METHANE FLOW UNDER VARYING LEVELS OF SOIL COMPACTION

M.M.T Lakshani^{1*}, T.K.K.C Deepagoda¹, T. J. Clough², J.R.R.N Jayarathne³, S. Thomas⁴, N. Balaine², B. Elberling⁵ and K. Smits³

¹Dept. of Civil Engineering, Faculty of Engineering, University of Peradeniya, 20400 Peradeniya, Sri Lanka

²Dept. of Soil and Physical Sciences, Lincoln University, P.O. Box 85084, Lincoln, 7647, New Zealand

³Dep. of Civil Engineering, Univ. of Texas, Arlington, TX 76019, USA

⁴Plant & Food Research Ltd. Gerald St, Lincoln 7608, New Zealand

⁵Department of Geosciences and Natural Resource Management, Center for Permafrost (CENPERM), University of Copenhagen, Øster Voldgade 10, DK-1350 Copenhagen, Denmark

*Correspondence E-mail: mmtharindilakshani@gmail.com, TP: +94713949728

Abstract: Soil density plays an important role in regulating the migration of greenhouse gases from terrestrial soils to the atmosphere. Soil moisture is one of the main soil physical control determining the fate and transport of gases in soils. This study investigated the transport of methane (CH₄) originating from a simulated CH₄ source within a variably compacted pasture soil. Simulations were carried out for dry and variably saturated soils. Steady-state methane flow was simulated as a density-dependant, multiphase flow considering a multicomponent mixture of CH₄, water vapour and air, under different soil moisture conditions. We used measured soil-water characteristic (SWC) and gas diffusivity data at five density levels (1.1, 1.2, 1.3, 1.4, and 1.5 Mg m⁻³) to parameterize predictive models. Permeability was estimated using an existing SWC-based saturated hydraulic conductivity function. Results show a distinct effect of soil density on CH₄ concentration profiles within the soil. Clear effects of soil moisture on CH₄ transport could also be seen in differentially compacted soils. Relatively smaller CH₄ concentrations were observed in dry soils where permeability, gas diffusivity and air-filled porosity were higher. With increasing density, the profile-accumulated concentrations > 0.3% increased up to 200 times under the dry condition. In moist soils, on the other hand, smaller air-filled porosity and higher moisture-controlled tortuosity resulted in reduced permeability and gas diffusivity, yielding high CH₄ concentrations in the soil profile with only a maximum five-fold increase in the accumulated concentration with increasing density.

Keywords: soil-gas diffusivity, soil compaction, soil moisture, methane transport, numerical modelling

1. Introduction

Methane (CH_4) is a potent greenhouse gas with a global warming potential of 28 over a 100-year time horizon, and a radiative forcing value, from 1750 to 2011, of $0.48 \pm 0.05 \text{ W m}^{-2}$ (Myhre et al. 2013). The atmospheric CH_4 concentration has increased by 150% since 1750 to be $1803 \pm 2 \text{ ppb}$ in 2011, increasing at $\sim 6 \text{ ppb yr}^{-1}$ between 2007 and 2011 (Hartmann et al. 2013). Furthermore, CH_4 is a chemically reactive molecule that plays an important role in atmospheric chemistry. Methane reacts with hydroxyl radicals in the atmosphere, reducing their oxidative potential and hence the atmosphere's ability to counteract anthropogenic pollutants, for example, chlorofluorocarbons (Montzka et al., 2011).

Methane sources may be broadly classified into three categories: biogenic, thermogenic, and pyrogenic. Atmospheric CH_4 is predominantly (70%-80%; Mer and Rogger, 2001) of biogenic origin, and stems largely from terrestrial ecosystems with environments favoring methanogens. Globally, it has been estimated (Ciais et al. 2013) that, between 2000 to 2009, rice paddy agriculture ($36 \text{ Tg CH}_4 \text{ yr}^{-1}$) and landfills ($75 \text{ Tg CH}_4 \text{ yr}^{-1}$) equated to approximately 33% of all anthropogenic CH_4 sources ($331 \text{ Tg CH}_4 \text{ yr}^{-1}$). Potentially, soils act as a CH_4 sink where aerobic conditions favor methanotrophy, leading to oxidation of atmospheric CH_4 (Gebert et al. 2011). Therefore, in order to better understand soil emissions of CH_4 , and their potential mitigation, a thorough understanding of the soil properties controlling CH_4 emissions under different environmental conditions is required.

Compaction-induced changes in soil structure essentially affect the transport and retention characteristics of both soil-water and soil-gas, and thereby affect the soil's potential for uptake and emission of greenhouse gases. Density-controlled effects on soil-water retention, gas diffusivity (D_p/D_o , where D_p and D_o are gas diffusion coefficients in soil and free air, respectively) (Croney and Coleman, 1954; Gupta et al., 1989) and hydraulic conductivity/permeability (Gent et al., 1983) have been highlighted in the literature; however, their impacts on the fate and transport of greenhouse gases (e.g., CH_4) have not been adequately studied.

The main objective of this study was to provide computational insight into the subsurface migration of CH_4 originating from a simulated CH_4 source located in differentially compacted soil systems under varied soil compaction, and moisture status. Soil physical measurements included soil bulk density, soil-water characteristic (SWC) and gas diffusivity, to estimate subsurface CH_4 concentrations in the absence of

measured concentration data. We test the hypothesis that soil moisture will considerably affect subsurface CH₄ in density-controlled soil systems.

2. Mathematical Modelling

2.1 Soil-Water Characteristic (SWC)

We used the van Genuchten (1980) model to characterize soil-water retention and parameterize the capillary suction (ψ)-soil moisture content (θ) relation as follows:

$$\theta(h) = \theta_r + (\theta_s - \theta_r) \left(\frac{1}{1 + |\alpha h|^n} \right)^m \quad (1)$$

where θ_s is the soil water content at saturation (cm³ cm⁻³), θ_r is the residual water content (cm³ cm⁻³), α is model scaling factor (cm⁻¹), and n and m are model shape factors. Although it is a common practice to constrain the shape factors by linking them together (e.g., $m = 1 - 1/n$; Muelem, 1986); in this study we treated both n and m as unconstrained/fitting parameters to obtain a better numerical fit to the measured data.

The maximum slope of the $\theta(h)$ function (Eq. 1) at the inflection point (i.e., at $d^2\theta/dh^2 = 0$) can be expressed by S as follows (Aschonitis et al., 2012);

$$S_i = -m^{1+m} n \alpha (\theta_s - \theta_r) (1 + m)^{-m-1} \quad (2)$$

2.2 Hydraulic Conductivity and Permeability

In the absence of measured hydraulic conductivity (m s⁻¹) data, several models are available in the literature to estimate hydraulic conductivity from basic and easy-to-measure soil physical properties. Aschonitis and Antonopoulos (2013), proposed an empirical hydraulic conductivity function based on the parameterized van Genuchten model linking to S (Eq. 2) which can be presented as:

$$K_s = 1632.5 |S| (3.9f)^{(-3.9f)} \quad (3)$$

$$f = \alpha \Phi_e$$

where Φ_e is the effective porosity (i.e., the total porosity minus the volumetric moisture content at a suction of -33 kPa; Ahuja et al., 1984) representing the pore space where water flow effectively occurs.

Intrinsic permeability, k , (m^2) of a porous medium can be computed from the hydraulic conductivity as follows:

$$K_s = k \frac{\rho g}{\eta} \quad (4)$$

Note that the saturated hydraulic conductivity is a function of the porous medium and the fluid properties which are denoted by the permeability (k , m^2) and fluidity ($\rho g/\eta$, $\text{m}^{-1}\text{s}^{-1}$), respectively.

2.3 Soil Gas Diffusivity (D_p/D_o)

Few predictive soil-gas diffusivity models account for the effect of soil density, although some models implicitly take the density effects into account via reduction in total porosity (e.g., Millington and Quirk, 1960 & 1961). Here we adopted a recent empirically based soil gas diffusivity model (Chamindu Deepagoda et al., 2018) that was developed, based on a previous predictive model, and calibrated against the same gas diffusivity data that we use in this study.

$$\frac{D_p}{D_o} = 0.4 \left(2 \left(\frac{\varepsilon}{\phi} \right)^{5.2} + 0.04 \left(\frac{\varepsilon}{\phi} \right) \right) \quad (5)$$

where the constant scale factors are best-fit values to the measured data.

2.4 Fate and Transport of Methane in Soil

For the governing equations (mass and energy balance, advective mass flux, and diffusive mass flux) relevant to the present study, the reader is referred to Chamindu Deepagoda et al. (2016).

3. Materials and Methods

We considered measured soil water characteristic (SWC) and gas diffusivity data from Balanine et al. (2016) to parameterize the models. The soil was sampled from a pasture site at Duncan Block ($43^\circ 38' 0.7''$ S, $172^\circ 29' 40''$ N), Lincoln, New Zealand. The soil was identified as a Templeton silt loam, Typic Immature Pallic under the New Zealand Soil Classification system (Hewitt, 1998). The soils, sampled at a depth of 15 cm, were air-dried and sieved (< 2 mm) prior to packing at five bulk density (ρ_b) levels: 1.1, 1.2, 1.3, 1.4, and 1.5 Mg m^{-3} . The samples were subsequently drained at 11 levels of matric potential (ψ); -1.0 , -1.5 , -2.0 , -3.0 , -4.0 , -5.0 , -6.0 , -7.0 , -8.0 , -9.0 , and -10 KPa. Soil-gas diffusivity (D_p/D_o) was measured at each matric potential

using a one-chamber diffusion apparatus (Taylor, 1949). All measurements were performed in triplicate. For detailed information on soil sampling, pre-treatments, and calculation procedures, the reader is referred to Balaine et al. (2016).

For numerical simulations, we used the multiphase transport simulator TOUGH2 (Pruess et al., 1999) together with the equation of state module EOS7CA (Oldenburg, 2015). TOUGH2/ EOS7CA can potentially simulate subsurface flow and transport of aqueous and gas phases containing up to five components (i.e., H₂O, brine, non-condensable gas (e.g., CH₄), gas tracer, and air) under isothermal or non-isothermal conditions.

A temperature corrected Fickian molecular diffusion coefficient was used to model methane gas diffusion. Henry's coefficients were estimated using the method described by Cramer (1982) to determine dissolution of CH₄ in the aqueous phase. Since the Henry's law approach formulated in the model is accurate for low pressure (< ~ 1 MPa) conditions, the model is essentially applicable to relatively shallow subsurface porous media systems (Oldenburg, 2015) as considered in this study. See Pruess et al. (1999) and Oldenburg (2015) for further information on the TOUGH2/EOS7CA model. In this study, simulations were carried out for both dry ($\theta = \theta_r$) and partially saturated conditions ($\theta = 0.30\text{-}0.50 \text{ cm}^3 \text{ cm}^{-3}$). We assumed that at each density level, homogeneous and isotropic conditions, with respect to transport parameters, prevailed across the entire domain.

Figure 1 shows the 2-D Cartesian computational domain used in the TOUGH2/EOS7A modelling framework for simulating CH₄ flow in the subsurface. A 10 m (width) x 0.15 m (height) numerical domain was discretised into 270 porous elements for simulations. The width of the domain (10 m) was selected based on the assumption that this width was large enough not to have boundary effects on flow simulations, while the height (0.15 m) represents the sampling depth. The left and right boundaries and the bottom boundary were treated as having no-flow conditions (Neumann-type) for gas flow and adiabatic conditions for heat transport, while the top boundary was considered as an open boundary for both mass and heat flows. A diffusive point CH₄ source was located at the mid-section of the domain 10 cm above the bottom boundary (Fig. 1) with a production rate converted to a flux of $9 \mu\text{mol m}^{-2} \text{ h}^{-1}$, an average value presented in literature (Oertel et al., 2016). Simulations were performed for both completely dry conditions (Fig. 1a) and for partially saturated conditions under a pre-defined soil moisture gradient (Fig. 1b). For partially saturated conditions, a pre-simulation was first performed to obtain the gravity-capillary equilibrium within the domain before applying the CH₄ flux.

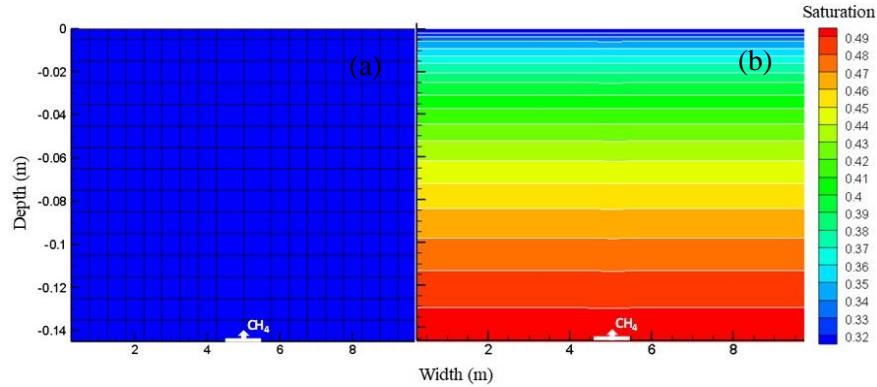


Figure 1: Discretised 2-D computational domains for methane migration simulations in (a) completely dry soil, and (b) partially saturated soil with a known soil moisture gradient. Location of the methane point diffusive source is also shown. Note different scales in X and Y axes.

3. Results and Discussion

Figure 2 shows the measured soil water-characteristic (SWC) in the pasture soil measured at five density levels. Note the systematic decline in saturated moisture content (θ_s) with increasing density, due to the drop in total porosity upon compaction. Compaction not only decreases the total volume of pores, but also causes a significant shift in dominant pore regions, thereby making an impact on pore size distribution. It is commonly accepted that compaction causes an increase in micropore (pore dia. $< 0.02 \mu\text{m}$), and mesopore ($0.02\text{-}30 \mu\text{m}$) regions, but decreases macropore ($> 30 \mu\text{m}$) domains (Yahya et al., 2011; Chamindu Deepagoda et al., 2018). Increases in the relative number of micro (or capillary) pores essentially increases the air-entry pressure/bubbling pressure (P_b) with increasing density, as also demonstrated in Fig. 2. The van Genuchten model (Eq. 1) provided a very good description of the measured data as shown by the solid lines. Note the slight disparity between measured and simulated data for 1.1 and 1.2 (Mg m^{-3}) density levels around 10 hPa matric suction, which is likely due to the aggregation of soil under low bulk density.

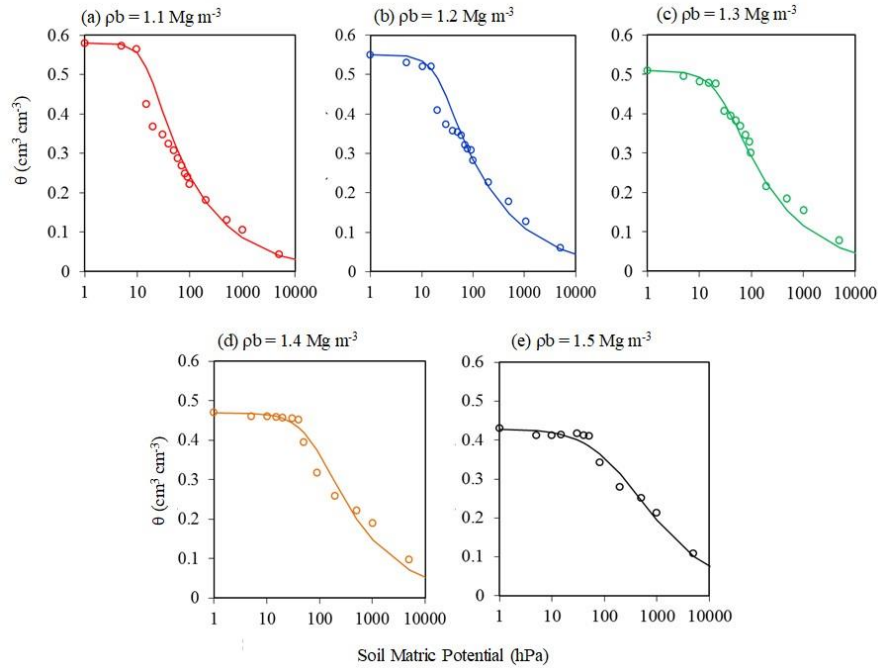


Figure 2: Measured soil-water characteristic data for pasture soil at different densities (in Mg m^{-3}): (a) 1.1, (b) 1.2, (c) 1.3, (d) 1.4, and (e) 1.5. Predictions from parameterized van Genuchten model (Eq. 1) are also shown (in solid lines). Note: $10 \text{ hPa} \approx 1 \text{ kPa}$.

The best-fit van Genuchten model parameters, together with the basic soil properties, are given in Table 1.

Table 1: Basic soil physical properties and parameterization

Bulk density Mg m^{-3}	Total porosity $\text{m}^3 \text{m}^{-3}$	Soil-Gas Diffusivity (dry soil)	Permeability [†] ($\times 10^{-12} \text{ m}^2$)	Soil-water characteristics Eq. (1)			
				θ_r	α	n	m
1.1	0.58	0.069	19.54	0	0.07	3	0.15
1.2	0.55	0.060	11.68	0	0.05	2.5	0.16
1.3	0.51	0.036	6.84	0	0.038	1.9	0.21
1.4	0.47	0.023	2.81	0	0.012	1.65	0.3
1.5	0.43	0.016	1.30	0	0.005	0.94	0.48

[†] Estimated from K_{sat} assuming a fluidity of $9.81 \times 10^6 \text{ m}^{-1} \text{ s}^{-1}$ at 20°C .

Another notable change in the SWC with the density is the change in slope of the curve at the inflection point, S (Eq. 2). A very good linear relationship ($r^2 = 0.95$) could be observed between the soil density and S (Fig. 3a), implying the applicability of S as a good indicator of the degree of soil densification/compaction, as evidenced also by previous studies (e.g., Aschonitis et al., 2012). Dexter (2004) also calculated the slope of the SWC at the inflection point (but expressed in a different form) and noted a linear decrease of slope (in non-aggregated soils) with increasing density. Dexter (2004) hypothesised the slope as a measure of microstructure that can be used as an index of soil physical quality. Figure 3(b) illustrates the variation of two dominant gas transport parameters with density: intrinsic permeability, k (m^2) (Eq. 3 & 4), and the soil-gas diffusion coefficient, D_s (m^2/s) (Eq. 5). Importantly, within the range of measured density, k varied over three orders-of-magnitude whereas the variation of D_s occurred within a single order-of-magnitude, while both parameters showing a decrease with increasing density. Since compaction causes the rearrangement of particles, and thereby changes the soil structure, the parameters which are predominantly soil structure controlled become mostly affected due to compaction. Also, air permeability, which characterizes the advective flow of gases in porous systems, is highly soil-structure-controlled, since advective gas flow occurs preferentially in macropore-dominant pore regions. As described earlier, compaction can cause a marked decrease in macropore density, yielding a remarkable drop in air permeability with increasing compaction. The soil-gas diffusion coefficient, on the other hand, is not predominantly controlled by the soil structure particularly under completely dry conditions, since diffusive gas flow occurs in all gas-accessible pore domains. However, due to the compaction-induced decrease in total porosity and increase in (solid-induced) tortuosity, a decrease in D_s can also be observed with increasing compaction.

It is worth mentioning that the soil gas transport properties need not necessarily be of equal importance across the entire soil system of interest. For example, if a gas is originating from a point source with a high pressure within the subsurface, the gas movement is more advective near the source and hence is controlled primarily by the air permeability. As the gas moves away from the source, the pressure decreases and therefore the flow becomes more diffusion-controlled, making gas diffusivity the controlling parameter. When the gas reaches the soil-atmosphere interface, the wind-induced near-surface pressure fluctuations may potentially make an advective gradient, thus making again the air permeability the controlling parameter. Further, the characteristics of the gas may also decide whether the dominant flow is advective or diffusive. For example, a low-density gas such as CH_4

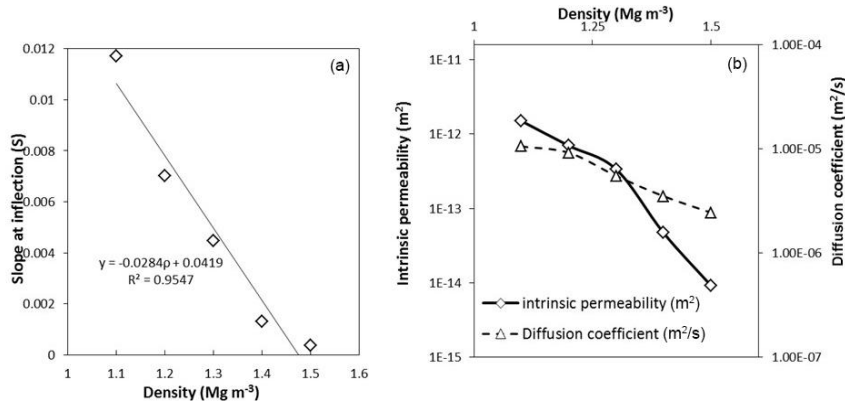


Figure 3:(a) Derived slope (Eq. 2) at the inflection point of the soil-water characteristic as a function of soil density. The best-fit linear regression line is also shown (in solid line). (b) Intrinsic permeability (k , Eq. 2) and soil gas diffusion coefficient (D_s , Eq 5). against soil density.

may preferentially move upward by advection (buoyancy) which is facilitated predominantly by the air permeability, with diffusion playing a minor role. Lateral CH₄ movement, however, occurs primarily by diffusion, and hence is controlled by gas diffusivity. In that respect, the anisotropy of the porous system with respect to the above transport properties is also of key concern in characterizing the gas flow in porous media.

Figure 4 shows the steady-state CH₄ concentration profiles for the five density levels for dry soils. The low density of CH₄ with respect to air causes density-driven advective flow which preferentially occurs upwards, leading to an upward-bulging CH₄ profile as can be seen at all density levels. The lateral and downward movements are only diffusion controlled. Note that due to the assumed isotropic conditions of soil regardless of compaction, diffusive movement is virtually the same in all directions at a given density. However, with increasing compaction, due to the marked decrease in total porosity, the diffusion coefficient and permeability (see Fig. 2b), the outward movement of CH₄ is constrained, increasing the mean residence time of methane in the soil profile, causing an increase in the CH₄ concentration and potential oxidation within the profile.

Simulated steady-state CH₄ concentration profiles for partially saturated conditions are shown in Fig. 5. The saturation contours, after simulations, are also shown (white colour). Methane concentration contours are distinctly different from those in dry soil systems (Fig. 4), demonstrating the clear effect of soil moisture on subsurface CH₄ dynamics. Note that the effect of

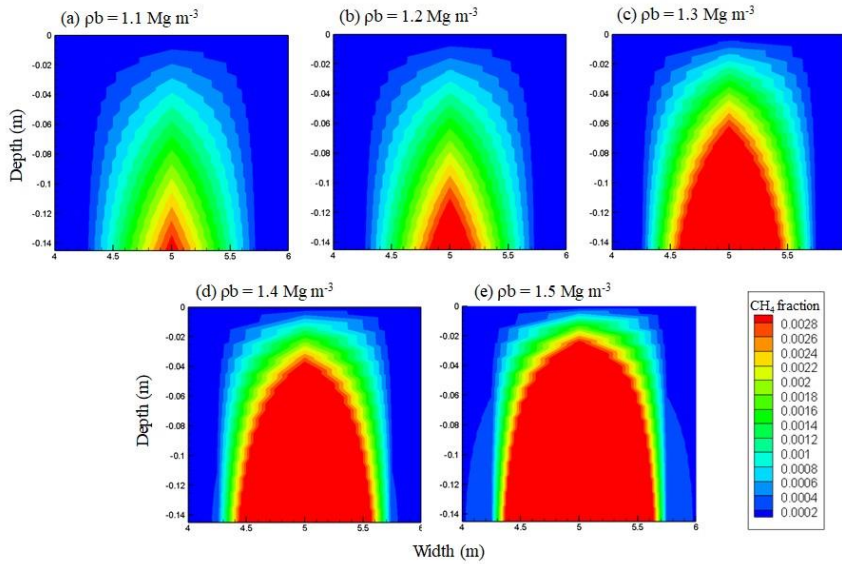


Figure 4: Simulated steady-state methane concentration maps for five soil density (ρ_b) levels for dry soils. Colours denote the mass fraction of gaseous methane.

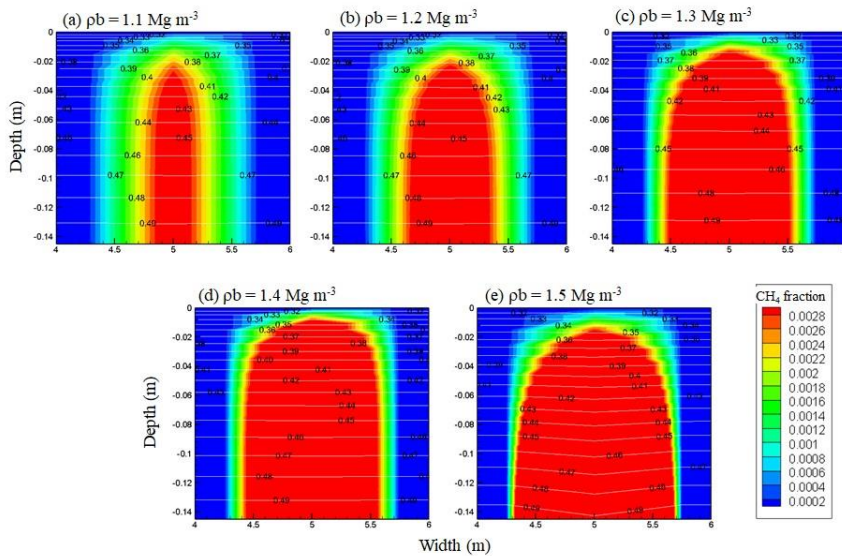


Figure 5: Simulated steady-state methane concentration maps for five soil density (ρ_b) levels for partially saturated soils with a predefined soil moisture gradient. Colours denote the mass fraction of gaseous methane. Soil moisture contours, after methane flow is applied, are denoted in white colour.

soil moisture on CH₄ concentration profiles is more evident at lower soil density (e.g., $\rho_b = 1.1 \text{ Mg m}^{-3}$) than high-density soil (e.g., $\rho_b = 1.5 \text{ Mg m}^{-3}$). Although the low-density soil has a larger air-filled pore space than the denser soils under the same moisture gradient, water held dominantly in micropores largely constrains movement of CH₄ through the gaseous phase, yielding a marked change in CH₄ concentration profiles in low density soil. In fact, the diffusion-controlled lateral movement of CH₄ varies more markedly, across density levels, under partially saturated condition (Fig. 5) as compared to buoyancy (advection)-dependent vertical movement, suggesting a clear effect of soil moisture on diffusive movement of CH₄ in the soil subsurface. Notably, the saturation contours are slightly distorted near the source in the higher-density soil ($\rho_b = 1.5 \text{ Mg m}^{-3}$) due to the inlet velocity allowing for a gaseous phase in otherwise fully saturated soil layers. Greatest variation of CH₄ accumulation is shown by dry conditions (see Fig. 4) with an approximate 200-fold accumulated area at the highest density (1.5 Mg m^{-3}) as compared to the lowest (1.1 Mg m^{-3}), with a systematic increase with increasing density. Accumulation CH₄ variation of under partially saturated condition, however, showed only a five-fold difference between the highest and the lowest densities. It is, therefore, clear that CH₄ accumulation within the profile is largely soil structure-controlled in the absence of soil moisture.

4. Conclusions

Based on measured soil-water characteristic (SWC), measured soil gas diffusivity, and derived permeability characteristics, we simulated CH₄ transport in five differently-compacted soils ($1.1 - 1.5 \text{ Mg m}^{-3}$) and determined the effects of soil moisture. Results showed a pronounced effect of soil density on subsurface CH₄ concentration profiles with enhanced concentrations in denser soils both for dry and partially saturated conditions. With increasing density (from 1.1 to 1.5 Mg m^{-3}), CH₄ concentration (above 0.3%) increased 200 times for dry soils, but only 5 times for partially saturated soils. The effect of soil moisture was observed to be more pronounced in less dense soils than in highly dense soils. Other environmental effects such as temperature, wind-induced atmospheric dynamics, porous media anisotropy, and CH₄ oxidation need to be considered in future simulation studies.

Acknowledgements

We gratefully acknowledge the funding from the Asia - Pacific Network for Global Change Research (APN) grant (CRRP2020-07MY-Deepagoda). The New Zealand Government and New Zealand

Agricultural Greenhouse Gas Research Centre (NZAGRC) under the Livestock Emissions and Abatement Research Network (LEARN) is also acknowledged.

References

- Ahuja, L.R., J.W. Naney, R.E. Green, and D.R. Nielsen. 1984. Macroporosity to characterize spatial variability of hydraulic conductivity and effects of land management. *Soil Sci. Soc. Am. J.* 48:699–702.
- Aschonitis, V.G., and V.Z. Antonopoulos. 2013. New equations for the determination of soil saturated hydraulic conductivity using the van Genuchten model parameters and effective porosity. *Irrig Drain* 62: 537-542.
- Aschonitis, V.G., S.K. Kostopoulou, and V.Z. Antonopoulos. 2012. Methodology to assess the effects of rice cultivation under flooded conditions on van Genuchten's model parameters and pore size distribution. *Transport Porous Med.* 91: 861-876.
- Balaine, N., T.J. Clough, M.H. Beare, S.M. Thomas, and E.D. Meenken. 2016. Soil gas diffusivity controls N₂O and N₂ emissions and their ratio. *Soil Sci. Soc. Am. J.* 80:529–540.
- Chamindu Deepagoda, T.K.K., Clough, T.J., Thomas, S., Balaine, N., Elberling, B., 2018. Density effects on soil-water characteristics, soil-gas diffusivity, and emissions of N₂O and N₂ from a re-packed pasture soil. *Soil Sci. Am. J.* doi: 10.2136/sssaj2018.01.0048.
- Chamindu Deepagoda T.K.K., K.M. Smits, and C.M. Oldenburg. 2016. Effect of subsurface soil moisture variability and atmospheric conditions on methane gas migration in shallow subsurface. *Int J Greenh Gas Control* 55:105–117.
- Ciais, P., C. Sabine, G. Bala, L. Bopp, V. Brovkin, J. Canadell, A. Chhabra, R. DeFries, J. Galloway, M. Heimann, C. Jones, C. Le Quéré, R.B. Myneni, S. Piao and P. Thornton. 2013. Carbon and Other Biogeochemical Cycles. In: *Climate Change 2013: The Physical Science Basis. Contribution of Working Group I to the Fifth Assessment Report of the Intergovernmental Panel on Climate Change* [Stocker, T.F., D. Qin, G.-K. Plattner, M. Tignor, S.K. Allen, J. Boschung, A. Nauels, Y. Xia, V. Bex and P.M. Midgley (eds.)]. Cambridge University Press, Cambridge, United Kingdom and New York, NY, USA.
- Conrad, R., H. Schfitz, and M. Babel. 1987. Temperature limitation of hydrogen turnover and methanogenesis in anoxic paddy soil. *FEMS Microbiol. Ecol.* 45: 281-289.

- Cramer, S D. Solubility of methane, carbon dioxide, and oxygen in brines from 0/sup 0/ to 300/sup 0/C. United States: N. p., 1982.
- Croney, D., J. D. Coleman. 1954. Soil structure in relation to soil suction (pF). *J. Soil Sci.* 5:75–84.
- Dexter, A.R. 2004. Soil physical quality Part I. Theory, effects of soil texture, density, and organic matter, and effects on root growth. *Elsevier: Geoderma*, 120: 201-214.
- Ehhalt D. H. and U. Schmidt. 1978. Sources and sinks of atmospheric methane. *Pure Appl. Geophys.* 116: 452–464.
- Gent, J.A., R. Ballard, and A.E. Hassan. 1983. The impact of harvesting and site preparation on the physical properties of lower coastal plain forest soils. *Soil Sci. Soc. Am. J.* 47:595–598.
- Gebert J., A. Groengroeft, and E.M. Pfeiffer. 2011, Relevance of soil physical properties for the microbial oxidation of methane in landfill covers. *Soil Biol Biochem* 43:1759–1767
- Gupta S C, P.P. Sharma, and S.A. Defranchi. 1989. Compaction effects on soil structure. *Adv. Agron.* 42: 311–338.
- Hartmann, D.L., A.M.G. Klein Tank, M. Rusticucci, L.V. Alexander, S. Brönnimann, Y. Charabi, F.J. Dentener, E.J. Dlugokencky, D.R. Easterling, A. Kaplan, B.J. Soden, P.W. Thorne, M. Wild and P.M. Zhai. 2013. *Observations: Atmosphere and Surface. In: Climate Change 2013: The Physical Science Basis.* Contribution of Working Group I to the Fifth Assessment Report of the Intergovernmental Panel on Climate Change [Stocker, T.F., D. Qin, G.-K. Plattner, M. Tignor, S.K. Allen, J. Boschung, A. Nauels, Y. Xia, V. Bex and P.M. Midgley (eds.)]. Cambridge University Press, Cambridge, United Kingdom and New York, NY, USA.
- Hewitt, A. E. & Manaaki Whenua-Landcare Research New Zealand Ltd. (1998). *New Zealand soil classification.* Lincoln, N.Z: Manaaki Whenua Press.
- Mer J.L., and P. Roger. 2001. Production, oxidation, emission and consumption of methane by soils: A review. *Eur J Soil Biol.* 37:25–50.
- Millington, R.J., and J.M. Quirk. 1960. Transport in porous media. p. 97–106. In F.A. Van Beren et al. (ed.) *Trans. Int. Congr. Soil Sci.*, 7th, Madison, WI. 14–21 Aug. 1960. Vol. 1. Elsevier, Amsterdam.
- Millington, R.J., and J.M. Quirk. 1961. Permeability of porous solids. *Trans. Faraday Soc.* 57:1200–1207.
- Montzka, S.A., E.J. Dlugokencky, and J.H. Butler. 2011. Non-CO₂ greenhouse gases and climate change. *Nature* 476: 43-50,
- Mualem, Y., 1986. Hydraulic conductivity of unsaturated soils: prediction and formulas. In: Klute, A. (Ed.), *Methods of Soil Analysis:*

- Part 1. Physical and Mineralogical Methods, 2nd. ed. *Am. Soc. Agron.*, Monograph, vol. 9, pp. 799 – 823.
- Myhre, G., D. Shindell, F.-M. Bréon, W. Collins, J. Fuglestedt, J. Huang, D. Koch, J.-F. Lamarque, D. Lee, B. Mendoza, T. Nakajima, A. Robock, G. Stephens, T. Takemura and H. Zhang. 2013: *Anthropogenic and Natural Radiative Forcing*. In: *Climate Change 2013: The Physical Science Basis*. Contribution of Working Group I to the Fifth Assessment Report of the Intergovernmental Panel on Climate Change [Stocker, T.F., D. Qin, G.-K. Plattner, M. Tignor, S.K. Allen, J. Boschung, A. Nauels, Y. Xia, V. Bex and P.M. Midgley (eds.)]. Cambridge University Press, Cambridge, United Kingdom and New York, NY, USA.
- [Oertel, C.](#), [J. Matschullat](#), [K. Zurba](#), [K. Zimmermann](#), and [S. Erasmí](#). 2016. Greenhouse gas emissions from soils - A review. *Soil Sci. Soc. Am. J.* 76: 327-352.
- Oldenburg, C.M., 2015. EOS7CA Version 1.0: *TOUGH2 Module for Gas Migration in Shallow Subsurface Porous Media Systems*, Lawrence Berkeley National Laboratory Report LBNL-175204.
- Parashar, D.C., P. K. Gupta, J. Rai, R.C. Sharma, and N. Singh. 1993. Effect of soil temperature on methane emission from paddy fields. *Chemosphere* 26: 247-250.
- Pruess, K., C.M. Oldenburg, and G.J. Moridis. 1999. *TOUGH2 User's Guide Version 2. E.O.* Lawrence Berkeley National Laboratory Report LBNL-43134.
- Schiitz, H., A. Holzapfel-Pschorn, R. Conrad, H. Rennenberg, and W. Seiler. 1989. A three-year continuous record on the influence of daytime, season and fertilizer treatment on methane emission rates from an Italian rice paddy field. *J. Geophys. Res.* 94: 405-416.
- Taylor, S.A. 1949. Oxygen diffusion in porous media as a measure of soil aeration. *Soil Sci. Soc. Am. Proc.* 14:55–6
- van Genuchten, M.Th. 1980. A closed-form equation for predicting the hydraulic conductivity of unsaturated soils. *Soil Sci. Soc. Am. J.* 44:892–89
- Yahya, Z., A. Husin, J. Talib, J. Othman, S. Z. Darus, O.H. Ahamed, and M.B. Jalloh. 2011. Pores Reconfiguration in Compacted Bernam Series *Soil. Am J Appl Sci.* 8: 212-216